Λ-Enhanced Imaging of Molecules in an Optical Trap

Editors' Suggestion | Featured in Physics

Λ-Enhanced Imaging of Molecules in an Optical Trap

Lawrence W. Cheuk,[1,2,*] Loïc Anderegg,[1,2] Benjamin L. Augenbraun,[1,2] Yicheng Bao,[1,2] Sean Burchesky,[1,2] Wolfgang Ketterle,[2,3] and John M. Doyle[1,2]

[1]*Department of Physics, Harvard University, Cambridge, Massachusetts 02138, USA*
[2]*Harvard-MIT Center for Ultracold Atoms, Cambridge, Massachusetts 02138, USA*
[3]*Department of Physics, Massachusetts Institute of Technology, Cambridge, Massachusetts 02139, USA*

(Received 31 May 2018; published 23 August 2018)

We report on nondestructive imaging of optically trapped calcium monofluoride molecules using *in situ* Λ-enhanced gray molasses cooling. 200 times more fluorescence is obtained compared to destructive on-resonance imaging, and the trapped molecules remain at a temperature of 20 μK. The achieved number of scattered photons makes possible nondestructive single-shot detection of single molecules with high fidelity.

DOI: 10.1103/PhysRevLett.121.083201

Ultracold molecules hold promise for many important applications, ranging from quantum simulation [1–4] and quantum information processing [5–9] to precision tests of fundamental physics [2,10–13]. Recently, direct laser cooling of molecules has seen rapid progress. Starting from the first demonstrations of magneto-optical traps (MOTs) [14–18], laser cooling to sub-Doppler temperatures, magnetic trapping and optical trapping of directly cooled molecules have all been achieved [19–21].

Applications in quantum simulation and information processing demand high-fidelity detection of the molecules, which has been a focus of recent work [22]. Other applications, including precision measurement, can also benefit from improved detection. Typically, fluorescence imaging of trapped ultracold samples is destructive due to recoil heating from photon scattering. In recent years, advanced imaging techniques for atoms have circumvented such heating, achieving sensitivities sufficient to detect single atoms. This has enabled quantum gas microscopy [23–27], which has provided unprecedented microscopic access into quantum many-body systems. Furthermore, nondestructive imaging has opened up new routes to prepare quantum states, as has been demonstrated recently in optical tweezer experiments [28–30].

In this Letter, we report on nondestructive imaging of optically trapped calcium monofluoride (CaF) molecules. We are able to scatter 2700 photons per molecule while keeping 90% of the molecules trapped at a temperature of 20 μK. This was not achievable in our earlier work using gray molasses cooling alone [18], and allows us to collect 200 times more photons as compared to standard on-resonance imaging. At the heart of our imaging method is a cooling technique known in the context of alkali atoms as Λ-enhanced gray molasses cooling. Despite a more complex internal structure in CaF, we have identified a scheme wherein Λ-enhanced cooling can be implemented, and have used it to cool molecules in free space to 5 μK, 10 times lower than previously reported. Λ-enhanced cooling has also enabled us to produce optically trapped samples that are 10 times higher in number and density, and 40 times higher in phase space density than previously reported [21].

As shown recently [17,21], sub-Doppler laser cooling of molecules can be achieved using gray molasses cooling, which relies on a Sisyphus cooling mechanism that appears at laser detunings to the blue of a $J \rightarrow J'(J' \leq J)$ transition [31–33]. In alkali atoms, gray molasses cooling can further be enhanced via a second mechanism that relies on velocity-dependent dark states created through two-photon resonances, a technique known as Λ-enhanced gray molasses [34]. This second mechanism, known as velocity-selective coherent population trapping (VSCPT), has been used in atoms to reach temperatures below a single photon recoil. VSCPT cooling can be described qualitatively by a three-level system with two ground states $|a\rangle$ and $|b\rangle$ addressed separately by two counterpropagating laser beams with two-photon detuning δ [Fig. 1(a)]. On two-photon resonance ($\delta = 0$), a dark state $(1/\sqrt{2})(|a\rangle - |b\rangle)$ that is decoupled from the laser light arises for a particle at rest. A particle moving at velocity v experiences a Doppler shift of the two-photon resonance of $2kv$, where k is the wave vector of the light, which couples dark states to bright states. After scattering multiple photons, particles accumulate in low-velocity states, since these are longer lived than high-velocity states [35–37]. In Λ-enhanced cooling, this mechanism is further helped by standard gray molasses cooling, which can operate outside the velocity range where VSCPT is effective. In alkali atoms, Λ-enhanced cooling typically cools to temperatures of a few photon recoils, much lower than possible with gray molassses cooling alone [32,34,38,39].

Implementing Λ cooling in molecules is more challenging than in alkali atoms because of their more complex internal structure. For example, in CaF, the relevant states for laser cooling are comprised of four ground state

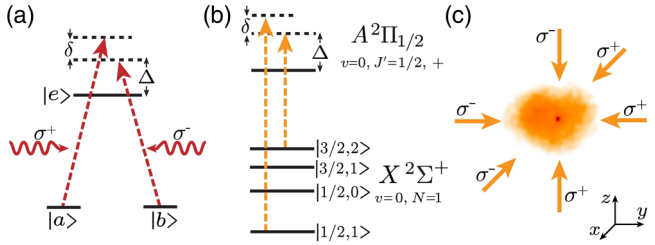

FIG. 1. (a) Three-level system exhibiting velocity-dependent dark states. Two ground states $|a\rangle$ and $|b\rangle$ are addressed separately by two counterpropagating laser beams. (b) Specific scheme for Λ cooling of CaF. The cooling light consists of two components addressing the $|J=1/2, F=1\rangle$ and $|3/2,2\rangle$ hyperfine manifolds. The single-photon detuning for $|1/2,1\rangle$ and two-photon detuning are denoted by Δ and δ, respectively. The hyperfine spacing between $|3/2,2\rangle$ and $|1/2,1\rangle$ is $h\times$ 73.160 MHz [40]. (c) Schematic of Λ-cooling beams, overlaid with a fluorescence image of Λ-cooled CaF molecules. Molecules in the optical dipole trap (ODT) appear as a bright spot surrounded by a larger cloud of untrapped molecules. [Λ imaging of trapped molecules is shown in Fig. 4(c).]

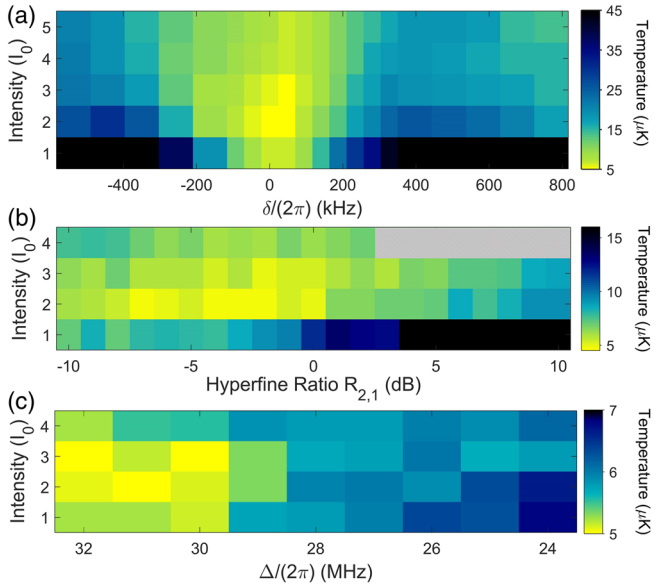

FIG. 2. Dependence of Λ cooling in free space on various parameters. (a) Temperature versus intensity I and two-photon detuning δ at fixed single-photon detuning ($\Delta=2.9\Gamma$) and hyperfine ratio ($R_{2,1}=0.92$). (b) Temperature versus I and $R_{2,1}$ with $\Delta=3.4\Gamma$ and $\delta=0$. $R_{2,1}$ is shown on a logarithmic scale, with the horizontal axis being 10 times the base-10 logarithm of the power ratios. (c) Temperature versus Δ and I with $R_{2,1}=0.92$ at $\delta=0$. For all plots, I was varied in steps of $I_0=6.8$ mW/cm^2.

hyperfine manifolds spaced by only a few excited state linewidths [Fig. 1(b)]. In contrast, alkali atoms have only two ground state hyperfine manifolds that are split by 10 s to 100 s of linewidths. Despite these molecular complications, we have identified a simple scheme in CaF.

The starting point of our experiment is a radio-frequency (rf) MOT of CaF loaded from a cryogenic buffer gas beam [18,21]. The MOT operates on the $X^2\Sigma^+(N=1)\rightarrow A^2\Pi_{1/2}(J'=1/2)$ transition and consists of three retroreflected beams containing four frequency components to address the various hyperfine manifolds [Fig. 1(b)], along with lasers to repump the ($Xv=1, 2, 3$) vibrational levels. The MOT beams are also used for Λ-enhanced cooling. After MOT loading, we switch off the MOT beams and the magnetic gradient in 200 μs, while simultaneously detuning the laser to $\Delta\approx 3$–4Γ, where $\Gamma=2\pi\times 8.3$ MHz is the excited linewidth [41]. The MOT beams, with polarization switching (required for the rf MOT) turned off, are then switched back on, but only with two frequency components nominally addressing the $|J,F\rangle=|3/2,2\rangle$ and $|1/2,1\rangle$ hyperfine manifolds [Fig. 1(b)].

Although only two frequency components nominally addressing $|3/2,2\rangle$ and $|1/2,1\rangle$ remain, all four hyperfine manifolds are still addressed. The $|3/2,2\rangle$ ($|3/2,2\rangle$) manifold is addressed directly by the $|1/2,1\rangle$ ($|1/2,1\rangle$) component. The $|3/2,1\rangle$ manifold is addressed by the $|3/2,2\rangle$ component, which is nearly resonant (blue detuned by $\sim 1\Gamma$) at this detuning Δ. This provides a Sisyphus cooling force. In addition, as a result of optical pumping, molecules spend only a small fraction of time in $|3/2,1\rangle$. To a first approximation, the $|3/2,1\rangle$ manifold can thus be ignored. For the $|1/2,0\rangle$ manifold, the $|3/2,2\rangle$ and $|1/2,1\rangle$ frequency components are detuned by 16Γ and -6Γ from resonance, respectively. Despite possible Sisyphus heating from the latter, this should be negligible since the $|1/2,0\rangle$ manifold has only one state.

Limiting to two the number of frequency components significantly reduces the parameter space that one must search for Λ-enhanced cooling. It also allows one to gain intuition from experiments with alkali atoms. We first vary the two-photon detuning δ and the total light intensity I. For all intensities used, we observe a temperature minimum near the two-photon resonance ($\delta=0$), with accompanying heating features when detuned [Fig. 2(a)]. Both the heating and cooling features become more pronounced at low intensities, which can be qualitatively explained by a three-level model. Away from resonance, the VSCPT dark states that are formed are at a finite velocity given by $\delta/(2k)$. Molecules accumulate in these longer-lived states at higher velocities, resulting in a higher average kinetic energy. We also observe that the width of the cooling feature increases with intensity, typical of VSCPT, where higher intensities increase the pumping rate into dark states. In a three-level model [Fig. 1(a)], the bright state admixture scales as $(\delta/\Omega)^2$, Ω being the single-photon Rabi frequency. Features that vary as a function of δ should broaden with increasing values of Ω^2. Since the intensity is proportional Ω^2, these features are expected to broaden with intensity, in agreement with our observations.

Previous demonstrations of Λ-enhanced cooling of alkali atoms have reported optimal cooling when the ratio of the

intensities of the hyperfine components is large [34,39]. Which of the components was stronger, however, was not found to be crucial [32]. In molecules, the dependence on the hyperfine ratio can be different because of additional hyperfine manifolds. We thus explore the dependence of Λ-enhanced cooling on $R_{2,1}$, the ratio of $|3/2,2\rangle$ light to $|1/2,1\rangle$ light. In contrast to observations in alkali atoms, we observe a strong asymmetry with respect to $R_{2,1}$ [Fig. 2(b)]. Optimal cooling occurs when $R_{2,1}$ is between 0.2 and 1.0, at a total intensity of $I \approx 14$ mW/cm^2. Cooling is much reduced when $R_{2,1} \gg 1$. One possible explanation is that while the $|1/2,1\rangle$ component is blue detuned relative to all hyperfine states and always provides Sisyphus cooling, the $|3/2,2\rangle$ component is red detuned relative to the $J = 1/2$ states and can cause Sisyphus heating.

After optimization of the temperature with respect to the single-photon detuning Δ and the total intensity I, we are able cool the molecules to 5.0(5) μK, 8 times colder than previously reported for gray molasses cooling alone [17,21]. We observe minimal dependence on Δ [Fig. 2(c)], and optimal cooling is achieved at $\Delta = 3.9\Gamma$, $I = 14\,\mathrm{mW/cm^2}$, $R_{2,1} = 0.92$, with an optimal two-photon detuning of $\delta_{\mathrm{opt,fs}} = 0$. With the measured free-space density of $1.4(3) \times 10^7$ cm^{-3}, the corresponding phase space density is $1.4(4) \times 10^{-8}$, 20 times higher than previously reported in free space [21].

The low temperature we achieved with Λ-enhanced cooling suggested that it could be used as an imaging technique for optically trapped molecules—one can collect spontaneously scattered photons while continuously cooling. Success of this approach depends on the efficacy of in-trap cooling, which is not a given, as differential Stark shifts between ground hyperfine states could destroy coherences needed for both Sisyphus cooling and VSCPT-like dark states.

We show here that although Stark shifts do have an effect, Λ cooling remains effective in an optical trap. To trap molecules, we use an optical dipole trap (ODT) formed by linearly polarized single-frequency 1064 nm light focused to a Gaussian beam waist of 29 μm and retroreflected with orthogonal polarization to ensure that no lattice structure in intensity is formed. At the trapping wavelength, the differential Stark shifts between ground hyperfine states are as large as ∼20% of the trap depth. These differential Stark shifts arise because of the nonzero tensor polarizability of the ground states relevant for laser cooling in $^2\Sigma$ molecules.

Since trap loading efficiency depends on the ability to laser cool in the trap [21], we first explore the dependence of trapped number versus two-photon detuning at different trap depths. We transfer molecules into the ODT by simultaneously turning on the ODT and the cooling light, which is initially at $\Delta = 2.9\Gamma$ and $I = 34$ mW/cm^2. This quickly ($1/e$ time of 1 ms) cools the samples down to ∼10 μK, significantly reducing the expansion due to finite temperature. After 1.5 ms, optimal free-space cooling parameters ($\Delta = 3.9\Gamma$, $I = 14$ mW/cm^2, $R_{2,1} = 0.92$) are used for the next 35 ms. The cooling light is then switched off for 50 ms to allow untrapped molecules to fall away before the number of trapped molecules is measured. As shown in Fig. 3(a), as a function of trap depth V, the optimal two-photon detuning for maximal trap loading, $\delta_{\mathrm{opt,trap}}$, is shifted from $\delta_{\mathrm{opt,fs}}$. The range in detuning for enhanced loading increases with V, and becomes broader than the free-space cooling feature [Fig. 2(a)]. The dependence of $\delta_{\mathrm{opt,trap}}$ on V at low depths is measured to be $+7.0(8) \times 10^{-2} \times (V/\hbar)$, and saturates when at $V \approx k_B \times 130$ μK. The shift in $\delta_{\mathrm{opt,trap}}$ is of the same scale as estimated differential Stark shifts between ground hyperfine states. The saturation of $\delta_{\mathrm{opt,trap}}$ with V might arise from the competition between optimal Λ cooling in free space and inside the trap. In deep traps, $\delta_{\mathrm{opt,trap}}$ can be shifted beyond the free-space cooling feature, reducing trap-loading efficiency.

In order to optimize for both free space and in-trap cooling, one can use higher intensities to broaden the Λ-enhanced cooling feature at the expense of minimum attained temperature [Fig. 2(a)]. To test this idea, we vary I and Δ with fixed V and δ [$V = k_B \times 130(10)$ μK, $\delta = \delta_{\mathrm{opt,trap}}$]. We find that the loaded number increases

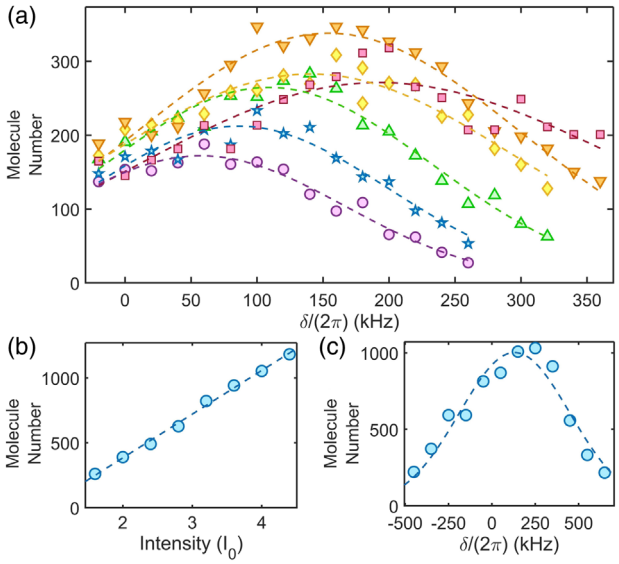

FIG. 3. (a) Number of molecules transferred into the ODT versus two-photon detuning δ at various trap depths V. With the exception of δ, Λ-cooling parameters are set to the free-space optimum ($\Delta = 3.9\Gamma$, $I = 14$ mW/cm^2, $R_{2,1} = 0.92$). Transferred number for different depths are shown in purple circles (trap depth of 30 μK), blue stars (50 μK), green upward triangles (60 μK), yellow diamonds (90 μK), orange downward triangles (130 μK), and red squares (160 μK). Dotted lines show fits to a skewed Gaussian curve. (b) Transferred number versus intensity I ($I_0 = 6.8$ mW/cm^2) at a trap depth of $V = k_B \times 130(10)$ μK. (c) Transferred number versus δ at a trap depth of $V = k_B \times 130(10)$ μK and intensity of $I = 31$ mW/cm^2. For all plots, $\Delta = 3.9\Gamma$ and $R_{2,1} = 0.92$.

with intensity [Fig. 3(b)], consistent with the idea that increased intensity reduces the sensitivity to δ, which also varies spatially in the trap due to differential Stark shifts. We find minimal dependence on Δ.

To verify that the two-photon resonance remains a key factor at high intensities, we measure the loaded number versus δ at the maximum intensity available ($I = 31$ mW/cm^2). As shown in Fig. 3(c), we observe a broad enhancement feature with a width in δ of $\sim 2\pi \times 1$ MHz. With optimized parameters [$\Delta = 3.9\Gamma$, $\delta = 2\pi \times 90$ kHz, $I = 31$ mW/cm^2, $V = 130(10)$ μK], 1300(160) molecules are transferred with a temperature of 21(3) μK, 3 times colder and 9 times higher in number than previously reported without Λ-enhanced cooling [21]. The peak trapped density of 6×10^8 cm^{-3} and phase space density of $8(2) \times 10^{-8}$ is 8 times and 40 times higher, respectively [21]. The significant improvement in transfer using Λ-enhanced cooling suggests that it remains effective in the trap.

To show that Λ cooling can be used for nondestructive detection, we first measure the trapped number as a function of cooling time. Molecules are loaded into the ODT using 150 ms of Λ cooling, which is then switched off for 50 ms to allow untrapped molecules to fall away. Λ cooling is subsequently applied for a variable time. To normalize out losses due to collisions with background gas, the samples are always held for the same total time. We find that the imaging lifetime is sensitive to $R_{2,1}$. At the optimal ratio ($R_{2,1} = 0.16$), the lifetime is 370(60) ms [Fig. 4(a)].

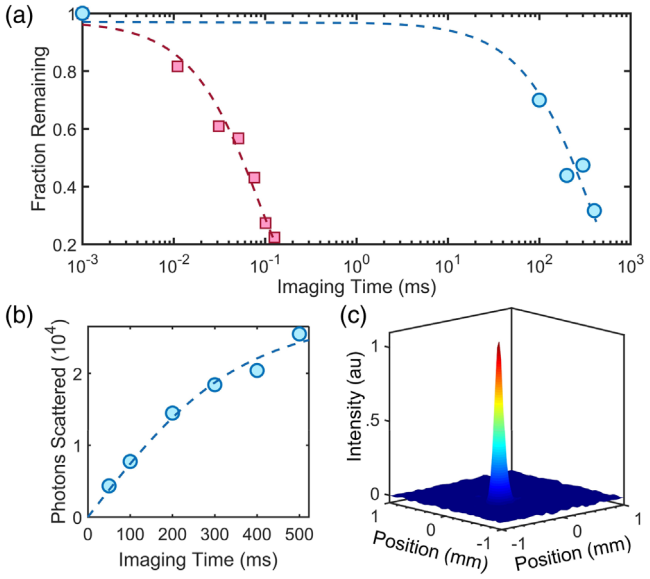

FIG. 4. (a) Fraction of molecules remaining versus imaging time for Λ imaging shown (blue circles) and resonant imaging (red squares). (b) Total number of photons scattered versus imaging time. (c) *In situ* Λ imaging of trapped molecules ($\Delta = 3.9\Gamma$, $\delta = 2\pi \times 90$ kHz, $I = 31$ mW/cm^2, and $R_{2,1} = 0.16$). The exposure time is 200 ms, and 50 individual images are averaged.

By comparing the collected fluorescence with that of resonant imaging, the scattering rate for Λ cooling is found to be $\Gamma_\Lambda = 70(10) \times 10^3$ s^{-1}. We can thus scatter 2700 (600) photons per molecule with 10% loss. With resonant imaging [scattering rate of $1.6(2) \times 10^6$ s^{-1}], the imaging lifetime is 80(5) μs [Fig. 4(a)], corresponding to the scattering of 13(2) photons per molecule with 10% loss. Λ imaging thus provides 200 times more photons. We also observe that even after 150 ms of Λ imaging, the molecular temperature is unchanged, staying at 20(3) μK, 6 times below the trap depth. In contrast, resonant fluorescent imaging applied for 60 μs increases the temperature to 50 μK and leads to significant losses.

A useful metric for detection is the imaging lifetime τ normalized by the scattering rate Γ_Λ, $\xi = \tau \times \Gamma_\Lambda$. Λ-enhanced imaging gives $\xi = 2.6(6) \times 10^4$. Two limiting mechanisms for ξ are branching into vibrational states not addressed by the available repumpers ($v = 1, 2, 3$), and mixing of $N = 3$ states into the nominal $N = 1$ states due to the hyperfine interaction. We determine from the MOT lifetime that both mechanisms will not limit ξ below 10^5. A separate loss mechanism is spatial diffusion during Λ cooling, which arises when Γ_Λ is much larger than the trap frequencies, which are $\omega_{x,y,z} = 2\pi \times (1.5 \times 10^3, 1.5 \times 10^3, 12)$ s^{-1} in our setup. This effect can be captured by a simple model where the velocity of a molecule is described by a Boltzmann distribution at a temperature of 20 μK, and randomized at the scattering rate Γ_Λ. A Monte Carlo simulation taking into account trap dynamics and gravity yields a lifetime of 700(100) ms, 2 times longer than observed. We believe that this model captures the dominant loss mechanism, and differences are likely explained by spatially inhomogeneous cooling. This diffusive loss could be reduced by lowering Γ_Λ at the expense of longer photon collection time.

With the imaging lifetime achieved here, a single-shot nondestructive readout of single molecules is now possible. In future experiments, where high photon collection efficiency can be obtained using a microscope objective, 10 s of photons per molecule can be detected with imaging losses in the 1% range. This projected photon number will be sufficient for high-fidelity detection of single molecules.

In conclusion, we have demonstrated nondestructive imaging of optically trapped CaF molecules using Λ-enhanced cooling. Despite complexities in the hyperfine structure, we have identified and implemented a scheme of Λ cooling that enables cooling to 5 μK in free space. This technique has significantly improved production of optically trapped samples, allowing trapping of 1300(160) molecules at a temperature of 21(3) μK and a peak density of $6(2) \times 10^8$ cm^{-3}. These densities are now sufficient for loading into arrays of optical tweezers, an emerging platform for quantum simulation and information processing [7–9,42–44]. Despite effects from differential Stark shifts, we have found Λ cooling to be effective in an optical trap.

By collecting scattered photons during Λ cooling, we are able to nondestructively detect trapped molecules. Compared to resonant fluorescent imaging, photon cycling is greatly enhanced, and 200 times more photons are emitted. Our imaging method opens the door to high-fidelity read out of single molecules and creation of defect-free molecular arrays [28–30]. The methods developed here are not specific to CaF, but are broadly applicable to other laser-coolable molecules (e.g. SrF, YbF, YO, YbOH, SrOH, CaOH, $CaOCH_3$), suitable for a wide variety of applications ranging from precision probes of particle physics [2,11–13] to ultracold chemistry [2,45,46]. For these applications, Λ imaging, which increases the number of scattered photons, will also be of significant help.

This work was supported by NSF. L. W. C. acknowledges support from Max Planck Harvard Research Center for Quantum Optics.

*lcheuk@g.harvard.edu

[1] A. Micheli, G. K. Brennen, and P. Zoller, Nat. Phys. **2**, 341 (2006).
[2] L. D. Carr, D. DeMille, R. V. Krems, and J. Ye, New J. Phys. **11**, 055049 (2009).
[3] G. Pupillo, A. Griessner, A. Micheli, M. Ortner, D.-W. Wang, and P. Zoller, Phys. Rev. Lett. **100**, 050402 (2008).
[4] H. P. Büchler, E. Demler, M. Lukin, A. Micheli, N. Prokof'ev, G. Pupillo, and P. Zoller, Phys. Rev. Lett. **98**, 060404 (2007).
[5] D. DeMille, Phys. Rev. Lett. **88**, 067901 (2002).
[6] S. F. Yelin, K. Kirby, and R. Côté, Phys. Rev. A **74**, 050301 (2006).
[7] J. A. Blackmore, L. Caldwell, P. D. Gregory, E. M. Bridge, R. Sawant, J. Aldegunde, J. Mur-Petit, D. Jaksch, J. M. Hutson, B. E. Sauer, M. R. Tarbutt, and S. L. Cornish, arXiv:1804.02372.
[8] K.-K. Ni, T. Rosenband, and D. D. Grimes, Chem. Sci. (2018), DOI: 10.1039/C8SC02355G.
[9] E. R. Hudson and W. C. Campbell, arXiv:1806.09659.
[10] ACME Collaboration, Science **343**, 269 (2014).
[11] D. M. Kara, I. J. Smallman, J. J. Hudson, B. E. Sauer, M. R. Tarbutt, and E. A. Hinds, New J. Phys. **14**, 103051 (2012).
[12] J. Lim, J. R. Almond, M. A. Trigatzis, J. A. Devlin, N. J. Fitch, B. E. Sauer, M. R. Tarbutt, and E. A. Hinds, Phys. Rev. Lett. **120**, 123201 (2018).
[13] I. Kozyryev and N. R. Hutzler, Phys. Rev. Lett. **119**, 133002 (2017).
[14] J. F. Barry, D. J. McCarron, E. B. Norrgard, M. H. Steinecker, and D. DeMille, Nature (London) **512**, 286 (2014).
[15] E. B. Norrgard, D. J. McCarron, M. H. Steinecker, M. R. Tarbutt, and D. DeMille, Phys. Rev. Lett. **116**, 063004 (2016).
[16] M. H. Steinecker, D. J. McCarron, Y. Zhu, and D. DeMille, ChemPhysChem **17**, 3664 (2016).
[17] S. Truppe, H. J. Williams, M. Hambach, L. Caldwell, N. J. Fitch, E. A. Hinds, B. E. Sauer, and M. R. Tarbutt, Nat. Phys. **13**, 1173 (2017).
[18] L. Anderegg, B. L. Augenbraun, E. Chae, B. Hemmerling, N. R. Hutzler, A. Ravi, A. Collopy, J. Ye, W. Ketterle, and J. M. Doyle, Phys. Rev. Lett. **119**, 103201 (2017).
[19] H. J. Williams, L. Caldwell, N. J. Fitch, S. Truppe, J. Rodewald, E. A. Hinds, B. E. Sauer, and M. R. Tarbutt, Phys. Rev. Lett. **120**, 163201 (2018).
[20] D. J. McCarron, M. H. Steinecker, Y. Zhu, and D. DeMille, Phys. Rev. Lett. **121**, 013202 (2018).
[21] L. Anderegg, B. L. Augenbraun, Y. Bao, S. Burchesky, L. W. Cheuk, W. Ketterle, and J. M. Doyle, Nat. Phys. (2018), DOI: 10.1038/s41567-018-0191-z.
[22] M. Zeppenfeld, Europhys. Lett. **118**, 13002 (2017).
[23] W. S. Bakr, J. I. Gillen, A. Peng, S. Flling, and M. Greiner, Nature (London) **462**, 74 (2009).
[24] J. F. Sherson, C. Weitenberg, M. Endres, M. Cheneau, I. Bloch, and S. Kuhr, Nature (London) **467**, 68 (2010).
[25] E. Haller, J. Hudson, A. Kelly, D. A. Cotta, B. Peaudecerf, G. D. Bruce, and S. Kuhr, Nat. Phys. **11**, 738 (2015).
[26] L. W. Cheuk, M. A. Nichols, M. Okan, T. Gersdorf, V. V. Ramasesh, W. S. Bakr, T. Lompe, and M. W. Zwierlein, Phys. Rev. Lett. **114**, 193001 (2015).
[27] M. F. Parsons, F. Huber, A. Mazurenko, C. S. Chiu, W. Setiawan, K. Wooley-Brown, S. Blatt, and M. Greiner, Phys. Rev. Lett. **114**, 213002 (2015).
[28] M. Endres, H. Bernien, A. Keesling, H. Levine, E. R. Anschuetz, A. Krajenbrink, C. Senko, V. Vuletic, M. Greiner, and M. D. Lukin, Science **354**, 1024 (2016).
[29] D. Barredo, S. de Léséleuc, V. Lienhard, T. Lahaye, and A. Browaeys, Science **354**, 1021 (2016).
[30] H. Bernien, S. Schwartz, A. Keesling, H. Levine, A. Omran, H. Pichler, S. Choi, A. S. Zibrov, M. Endres, M. Greiner, V. Vuleti, and M. D. Lukin, Nature (London) **551**, 579 (2017).
[31] G. Grynberg and J.-Y. Courtois, Europhys. Lett. **27**, 41 (1994).
[32] F. Sievers, N. Kretzschmar, D. R. Fernandes, D. Suchet, M. Rabinovic, S. Wu, C. V. Parker, L. Khaykovich, C. Salomon, and F. Chevy, Phys. Rev. A **91**, 023426 (2015).
[33] J. A. Devlin and M. R. Tarbutt, New J. Phys. **18**, 123017 (2016).
[34] A. T. Grier, I. Ferrier-Barbut, B. S. Rem, M. Delehaye, L. Khaykovich, F. Chevy, and C. Salomon, Phys. Rev. A **87**, 063411 (2013).
[35] A. Aspect, E. Arimondo, R. Kaiser, N. Vansteenkiste, and C. Cohen-Tannoudji, Phys. Rev. Lett. **61**, 826 (1988).
[36] J. Lawall, F. Bardou, B. Saubamea, K. Shimizu, M. Leduc, A. Aspect, and C. Cohen-Tannoudji, Phys. Rev. Lett. **73**, 1915 (1994).
[37] J. Lawall, S. Kulin, B. Saubamea, N. Bigelow, M. Leduc, and C. Cohen-Tannoudji, Phys. Rev. Lett. **75**, 4194 (1995).
[38] A. Burchianti, G. Valtolina, J. A. Seman, E. Pace, M. De Pas, M. Inguscio, M. Zaccanti, and G. Roati, Phys. Rev. A **90**, 043408 (2014).

[39] G. Colzi, G. Durastante, E. Fava, S. Serafini, G. Lamporesi, and G. Ferrari, Phys. Rev. A **93**, 023421 (2016).
[40] W. J. Childs, G. L. Goodman, and L. S. Goodman, J. Mol. Spectrosc. **86**, 365 (1981).
[41] T. E. Wall, J. F. Kanem, J. J. Hudson, B. E. Sauer, D. Cho, M. G. Boshier, E. A. Hinds, and M. R. Tarbutt, Phys. Rev. A **78**, 062509 (2008).
[42] N. Schlosser, G. Reymond, and P. Grangier, Phys. Rev. Lett. **89**, 023005 (2002).
[43] D. D. Yavuz, P. B. Kulatunga, E. Urban, T. A. Johnson, N. Proite, T. Henage, T. G. Walker, and M. Saffman, Phys. Rev. Lett. **96**, 063001 (2006).
[44] L. R. Liu, J. D. Hood, Y. Yu, J. T. Zhang, N. R. Hutzler, T. Rosenband, and K.-K. Ni, Science **360**, 900 (2018).
[45] R. V. Krems, Phys. Chem. Chem. Phys. **10**, 4079 (2008).
[46] I. Kozyryev, L. Baum, K. Matsuda, and J. M. Doyle, ChemPhysChem **17**, 3641 (2016).